

**MODEL FOR ENERGY TRANSFER IN THE SOLAR WIND:  
FORMULATION OF MODEL**

*R. E. Hartle and Aaron Barnes*

**ABSTRACT** On the basis of conclusions drawn from previous experimental and theoretical evidence, we extend the two-fluid solar-wind model by including the collisionless dissipation of hydromagnetic waves originating at the sun. We generate a series of solar wind models parameterized by the total energy flux of hydromagnetic waves at the base of the model. The resulting properties of propagation and dissipating of hydromagnetic waves on this model are presented.

We interpret the strong positive correlation between observed solar wind speeds  $v_E$  (subscript  $E$  refers to values at 1 AU) and proton temperatures  $T_{pE}$  [Burlaga and Ogilvie, 1970; Hundhausen et al., 1970] as defining a continuum of average macroscopic states. In this case, a realistic model of the wind should be capable of predicting a continuous range of wind speeds and proton temperatures consistent with this  $T_{pE}$ - $v_E$  correlation. Since the wind is frequently observed to blow much faster than the "quiet day" wind, it convects much more energy at some times than at others. We believe that this variability in energy flux reflects the dissipation of varying amounts of nonthermal energy supplied to the system, a view consistent with the  $T_{pE}$ - $v_E$  correlation.

On this basis, we have recently shown [Hartle and Barnes, 1970], in the context of the two-fluid model [Sturrock and Hartle, 1966; Hartle and Sturrock, 1968] that it is possible to choose, *ad hoc*, a class of hypothetical energy deposition functions that give models consistent with the  $T_{pE}$ - $v_E$  correlation. Accordingly, we found that primary energy deposition occurs over an extended region up to about  $25 R_\odot$  from the sun. This result is compatible with the nonthermal heating mechanism suggested by Barnes [1968, 1969];

that is, the collisionless dissipation of fast-mode hydromagnetic waves originating at the sun.

Here we extend our previous model by replacing the artificial heat source with that corresponding to hydromagnetic dissipation. We present some of the properties of propagation and dissipation of hydromagnetic waves as found from a self-consistent treatment of the two-fluid equations with such heating.

This treatment is simplified by assuming that the solar wind is composed of protons and electrons which undergo steady, radial, spherically symmetric expansion. The flow is then described in terms of the proton density  $n$  and flow speed  $v$  (equal to electron density and flow speed), the electron temperature  $T_e$ , and the proton temperature  $T_p$  as functions of the heliocentric distance  $r$ . These profiles are determined by the two-fluid equations of continuity, momentum, and energy given in Hartle and Barnes [1970] by

$$nvr^2 = J = \text{constant} \tag{1}$$

$$nm_p v \frac{dv}{dr} = -\frac{d}{dr} [nk(T_e + T_p)] - \frac{GM_\odot m_p n}{r^2} \tag{2}$$

$$\frac{3}{2} n v k \frac{dT_e}{dr} - v k T_e \frac{dn}{dr} - \frac{1}{r^2} \frac{d}{dr} \left( r^2 \kappa_e \frac{dT_e}{dr} \right) = -\frac{3}{2} v_E n k (T_e - T_p) + \mathcal{P}_e \tag{3}$$

---

*The authors are with the NASA Laboratory for Planetary Atmospheres, Goddard Space Flight Center, Greenbelt, Md., and the Space Science Division, Ames Research Center, Moffett Field, California.*

$$\frac{3}{2} nvk \frac{dT_p}{dr} - vkT_p \frac{dn}{dr} - \frac{1}{r^2} \frac{d}{dr} \left( r^2 \kappa_p \frac{dT_p}{dr} \right) = \frac{3}{2} \nu_E nk (T_e - T_p) + \mathcal{P}_p \quad (4)$$

in terms of the proton and electron masses  $m_p$  and  $m_e$ , the solar mass  $M_\odot$ , the gravitational constant  $G$ , and Boltzmann's constant  $k$ . The electron and proton thermal conduction coefficients,  $\kappa_e$  and  $\kappa_p$ , and the electron-proton energy exchange rate  $\nu_E$  are those of *Braginskii* [1965]. The fast-mode hydromagnetic heat sources are of the form

$$\mathcal{P}_{(e)}^{(p)}(r) = \int d^3k \mathcal{P}_{(e)}^{(p)}(k, r) \quad (5)$$

$$\mathcal{P}_{(e)}^{(p)}(k, r) = (\omega_0 - \mathbf{k} \cdot \mathbf{v}) W(k, r) G_{(e)}^{(p)} \left( \frac{\omega_0 - \mathbf{k} \cdot \mathbf{v}}{k}, e_{\mathbf{k}}, r \right) \quad (6)$$

The local plasma-frame (complex) circular frequency, in terms of the rest-frame (of the sun) frequency  $\omega_0$  and wave vector  $\mathbf{k}$ , is given by  $\bar{\omega} = \omega + i\gamma = \omega_0 - \mathbf{k} \cdot \mathbf{v} + i\gamma$  and is related to  $\mathbf{k}$  through the dispersion relation [Barnes, 1968]. The factor  $W$  is the energy density spectrum of the waves and  $G$  corresponds to the energy absorption by the protons (electrons) per unit wave energy in the time  $1/\omega$ . The heat functions are based on the assumptions that the velocity distributions are Maxwellian, that the wave amplitudes are small enough that linear wave theory is valid, and that  $|\gamma| \ll \omega$ .

The energy deposition term  $G_{(e)}^{(p)}$  is a complicated

function of the plasma parameters  $n$ ,  $\mathbf{v}$ ,  $T_e$ , and  $T_p$ , the local average magnetic field  $\mathbf{B}(r)$ , and the angle  $\theta$  between the wave vector  $\mathbf{k}$  and field  $\mathbf{B}$ . We assume that the average properties of the magnetic field  $\mathbf{B}(r)$  are adequately described by the spiral model of *Parker* [1963]. In the models considered here, the electron energy deposition term  $G_e \approx 0$  since the electron-electron collision frequency is much greater than the source frequency  $\omega_0 = 2 \times 10^{-2} \text{ sec}^{-1}$  (see below). The typical dependence of the proton energy deposition term  $G_p$  on  $\theta$  is shown in figure 1 for plasma parameters at the base of one of the models (see below;  $F_0 = 5.2 \times 10^3 \text{ ergs cm}^{-2} \text{ sec}^{-1}$  for this case). Here we note that the energy deposition distribution peaks at  $\theta \sim 20^\circ$  and that primary proton heating occurs over the range  $10^\circ \lesssim \theta \lesssim 35^\circ$ .

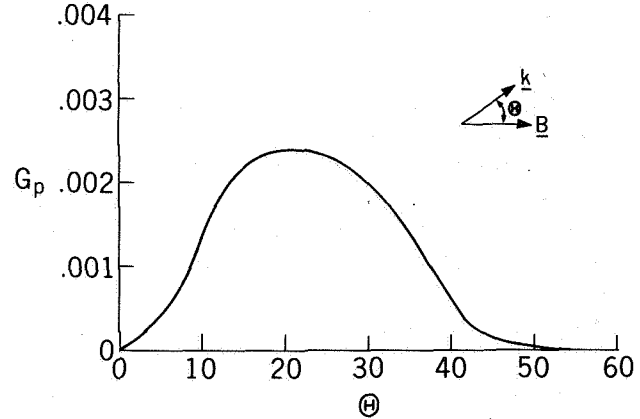


Figure 1. Proton energy absorption rate per unit wave energy in time  $1/\omega$  versus  $\theta$ , the angle between the wave vector and magnetic field.

Since the wavelengths in question are small relative to macroscopic scale lengths, we determine the energy density  $W$  of the waves in the approximation of "geometrical hydromagnetics." In this case, the ray paths  $\mathbf{x}(s)$  and wave vectors  $\mathbf{k}(s)$  ( $s$  is path length along ray) are obtained from Hamilton's equations, the dispersion relation, and the computed profiles  $n$ ,  $\mathbf{v}$ ,  $T_p$ ,  $T_e$ , and  $\mathbf{B}$ . Then for a given pair  $(\mathbf{x}_0, \mathbf{k}_0)$  at the base and fixed  $\omega_0$

$$W[\mathbf{k}(s), \mathbf{x}(s)] = W(\mathbf{k}_0, \mathbf{x}_0) \exp \int_{s_0}^s \frac{2\gamma_{\mathbf{k}}(s')}{|\partial\omega(s')/\partial\mathbf{k}|} ds' \quad (7)$$

where  $\gamma_{\mathbf{k}} = \text{Im } \omega_{\mathbf{k}}$  is the damping decrement and  $\partial\omega/\partial\mathbf{k}$  the group velocity, and the integration is along the ray.

The solar-wind models considered here are determined by self-consistent numerical solutions of equations (1) through (7) and the ray equations using a method of iteration similar to that described in *Hartle and Barnes* [1970]. In addition to specifying the magnetic field strength  $B_0$  and the hydromagnetic wave spectrum at the base of the model, the solutions are subject to the usual constraints of specifying the base density and temperatures  $n_0$ ,  $T_{e0}$ ,  $T_{p0}$ , requiring the velocity  $\mathbf{v}$  to pass continuously through the subsonic-supersonic transition, and requiring  $T_e$  and  $T_p$  to tend to zero as  $r$  goes to infinity. We treat the wave spectrum as a discrete number of rays (six in this work), weighted so that the base intensity is approximately isotropic in the outward directions (zero in the inward directions), and the frequency spectrum is assumed monotonic. The boundary values we choose at the base

$r = 2R_{\odot}$  are  $n_0 = 1.5 \times 10^6 \text{ cm}^{-3}$ ,  $T_{e0} = 1.3 \times 10^6 \text{ }^{\circ}\text{K}$ ,  $T_{p0} = 1.7 \times 10^6 \text{ }^{\circ}\text{K}$ , and  $B_0 = 0.18$ , consistent with coronal observations [Newkirk, 1967]. Our selection  $T_{p0} > T_{e0}$ , implying selective proton heating below the base, is consistent with the inner corona heating model of D'Angelo [1968, 1969]. The source frequency is taken to be  $\omega_0 = 2 \times 10^{-2} \text{ sec}^{-1}$ , near the peak of the observed photospheric and chromospheric acoustic spectrum [Leighton et al., 1962; Tanenbaum et al., 1969].

We have calculated a series of models that are parameterized by the remaining free parameter of the system; namely, the total energy flux  $F_0$  of hydromagnetic waves at the base. Three of the resulting ray trajectories are shown in figure 2 in terms of their azimuthal and radial coordinates  $\phi$  and  $r/R_{\odot}$ . These trajectories, corresponding to a flux  $F_0 = 5.2 \times 10^3 \text{ ergs cm}^{-2} \text{ sec}^{-1}$ , are typical of the class of models we considered and, for purposes of illustration, have been selected so that they all become radial at  $\phi = 0$ . The base emission angles  $\theta_e \equiv \cos^{-1}(\mathbf{k} \cdot \hat{r}/k)$ , between the wave vectors and the radial direction, are  $0^{\circ}$ ,  $15^{\circ}$ , and  $45^{\circ}$ . We note that the ray with emission angle  $\theta_e = 0$  propagates radially while the remaining rays refract toward the radial direction, becoming essentially radial at 10 or  $12 R_{\odot}$ . In addition, we observe that the refraction becomes stronger as the emission angle increases.

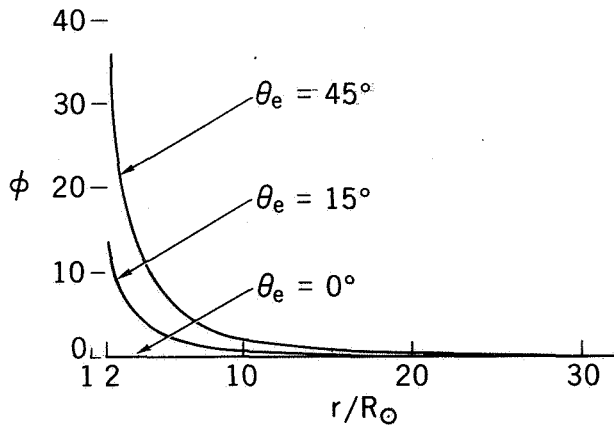


Figure 2. Ray trajectories in equatorial plane.

Let us now consider the damping of these rays. The peak amplitude of the energy deposition term  $G_p$  increases strongly with  $\beta_p = 8\pi nkT_p/B^2$ ; for example, the damping rate  $\gamma \propto \exp(-1/\beta_p)$  when  $\beta_p \lesssim 0.1$ . Nevertheless, since the shape of the energy deposition term  $G_p$  of figure 1 is essentially the same for the range of parameters of interest, we can get a qualitative

indication of where the relative damping between rays takes place by considering the angles  $\theta$  each wave vector makes with the magnetic field. The  $\theta$  profiles corresponding to the rays of figure 2 are shown in figure 3. In this case, the ray with emission angle  $\theta_e = 45^{\circ}$  should lose a significant portion of its energy at radii less than about  $6 R_{\odot}$  since it passes through the range  $10^{\circ} < \theta < 35^{\circ}$  where the damping is strongest (damping will be relatively weak for  $r \lesssim 2.5 R_{\odot}$ ). The intermediate ray,  $\theta_e = 15^{\circ}$ , will not damp as strongly near the base, resulting in a more extended heating region. Finally, the radial ray corresponds to the most extended dissipation since it has relatively low values of  $\theta$  throughout. The rays dissipate at similar rates beyond about  $12 R_{\odot}$  where they are essentially radial. In this region  $\theta$  increases with the spiral angle, resulting in increasing deposition rates with  $r$ ; here the remaining portion of the wave energy is lost.

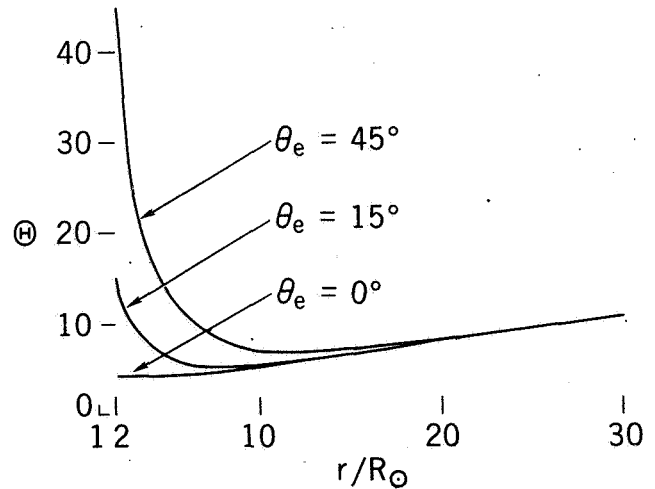


Figure 3. Angle  $\theta$  between the wave vector and magnetic field versus radial position  $r/R_{\odot}$ .

Upon summing the heat contribution from each ray we obtain the proton heat source  $P_p$  on this model. The resulting energy deposition distributions are shown in figure 4 corresponding to three models with  $F_0 = 2.2 \times 10^3$ ,  $5.2 \times 10^3$ , and  $1.2 \times 10^4 \text{ (ergs cm}^{-2} \text{ sec}^{-1})$ , which result in wind speeds  $v_E = 290$ ,  $370$ , and  $427 \text{ (km sec}^{-1})$  and proton temperatures  $T_{pE} = 2 \times 10^4$ ,  $6.2 \times 10^4$ , and  $1.7 \times 10^5 \text{ (}^{\circ}\text{K)}$ , respectively. These models are consistent with the  $T_{pE} - v_E$  correlation as discussed earlier by Barnes and Hartle (p. 219). For clarity, we normalized the heat profiles by the density to give the heating rate per proton. In each model hydromagnetic heating is important over an extensive region of  $20\text{--}30 R_{\odot}$  in radius. Beyond this region,  $P_p$  decays

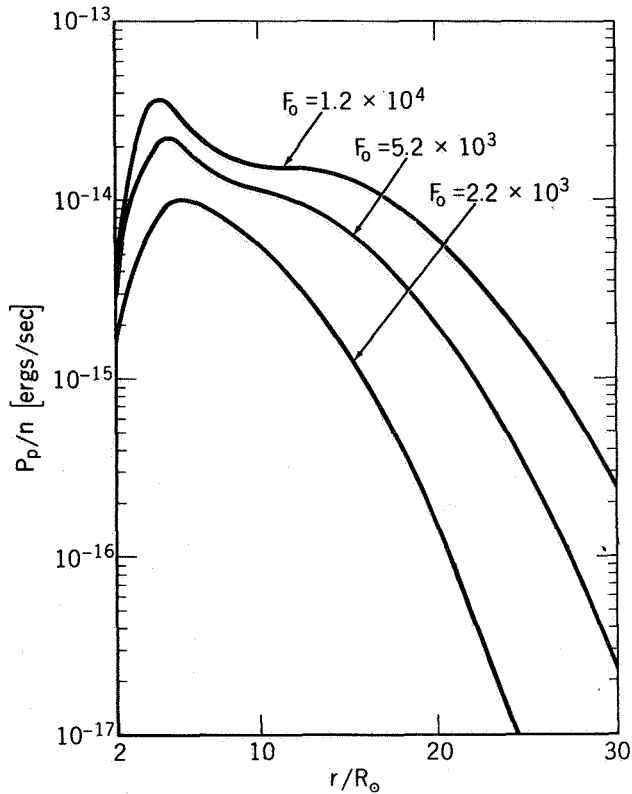


Figure 4. Normalized proton heat sources  $P_p/n$  versus radial position  $r/R_\odot$ .

rapidly and other terms in the proton heat equation become dominant.

When the energy flux  $F_0$  is increased, we note in figure 4 that there is an overall increase in the heat profile resulting in both increased wind speeds  $v_E$  and proton temperatures  $T_{pE}$  at 1 AU. This is consistent with our previous model [Hartle and Barnes, 1970], which demonstrated that heating in the region of subsonic flow ( $r \lesssim 5-7 R_\odot$ ) primarily raises the wind speed at 1 AU and heating in the supersonic flow region primarily raises the proton temperature at 1 AU. Also consistent with a requirement of our previous model is the inward motion of the heat source peak with increasing flux  $F_0$ . This variation in the peak is related to the fact that increased heating raises  $\beta_p = 8\pi nkT_p/B^2$ , which in turn raises the damping rate  $\gamma \propto \exp(-1/\beta_p)$ , leading to a relatively larger rate of energy deposition near the base.

#### REFERENCES

- Barnes, A.: Collisionless Heating of the Solar-Wind Plasma, I, Theory of the Heating of Collisionless Plasma by Hydromagnetic Waves. *Astrophys. J.*, Vol. 154, 1968, p. 751.
- Barnes, A.: Collisionless Heating of the Solar-Wind Plasma, II, Application of the Theory of Plasma Heating by Hydromagnetic Waves. *Astrophys. J.*, Vol. 155, 1969, p. 311.
- Braginskii, S. I.: Transport Processes in a Plasma, in *Reviews of Plasma Physics*, Vol. 1, edited by M. A. Leontovich, Consultants Bureau, New York, 1965, p. 205.
- Burlaga, L. S.; and Ogilvie, K. W.: Heating of the Solar Wind. *Astrophys. J.*, Vol. 159, 1970, p. 659.
- D'Angelo, N.: Heating of the Solar Corona. *Astrophys. J.*, Vol. 154, 1968, p. 401.
- D'Angelo, N.: Heating of the Solar Corona. *Solar Phys.*, Vol. 7, 1969, p. 321.
- Hartle, R. E.; and Sturrock, P. A.: Two-Fluid Model of the Solar Wind. *Astrophys. J.*, Vol. 151, 1968, p. 1155.
- Hartle, R. E.; and Barnes, A.: Nonthermal Heating in the Two-Fluid Solar Wind Model. *J. Geophys. Res.*, Vol. 75, 1970, p. 6915.
- Hundhausen, A. J.; Bame, S. J.; Asbridge, J. R.; and Sagdorak, J.: Solar Wind Proton Properties: Vela 3 Observations from July 1965-June 1967. *J. Geophys. Res.*, Vol. 75, 1970, p. 4643.
- Leighton, R. B.; Noyes, R. W.; and Simon, G. W.: Velocity Fields in the Solar Atmosphere, I, Preliminary Rep. *Astrophys. J.*, Vol. 135, 1962, p. 474.
- Newkirk, G., Jr.: Structure of the Solar Corona, in *Annual Review of Astronomy and Astrophysics*, Vol. 5, edited by L. Goldberg, D. Layzer, and J. G. Phillips, Annual Reviews, Inc., Palo Alto, Calif., 1967, p. 213.
- Parker, E. N.: *Interplanetary Dynamical Processes*. Interscience, New York, 1963.
- Sturrock, P. A.; and Hartle, R. E.: Two-Fluid Model of the Solar Wind. *Phys. Rev. Letters*, Vol. 16, 1966, p. 628.
- Tanenbaum, A. S.; Wilcox, J. M.; Frazier, E. N.; and Howard, R.: Solar Velocity Fields: 5-min Oscillations and Supergranulation. *Solar Phys.*, Vol. 9, 1969, p. 328.